



Fermi National Accelerator Laboratory

FERMILAB-Conf-95/218-E

D0

**Rapidity Correlations Between High p_T Intermediate Vector Bosons
and Jets in $\bar{p}p$ Collisions at $\sqrt{s} = 1.8$ TeV**

S. Abachi et al.

The D0 Collaboration

*Fermi National Accelerator Laboratory
P.O. Box 500, Batavia, Illinois 60510*

July 1995

Submitted to the *International Europhysics Conference on High Energy Physics (HEP95)*,
Brussels, Belgium, July 27-August 2, 1995

Disclaimer

This report was prepared as an account of work sponsored by an agency of the United States Government. Neither the United States Government nor any agency thereof, nor any of their employees, makes any warranty, expressed or implied, or assumes any legal liability or responsibility for the accuracy, completeness, or usefulness of any information, apparatus, product, or process disclosed, or represents that its use would not infringe privately owned rights. Reference herein to any specific commercial product, process, or service by trade name, trademark, manufacturer, or otherwise, does not necessarily constitute or imply its endorsement, recommendation, or favoring by the United States Government or any agency thereof. The views and opinions of authors expressed herein do not necessarily state or reflect those of the United States Government or any agency thereof.

Rapidity Correlations Between High p_T Intermediate Vector Bosons and Jets in $\bar{p}p$ Collisions at $\sqrt{s} = 1.8$ TeV

The DØ Collaboration¹
(July 1995)

DØ has used $W \rightarrow e\nu$ and $Z \rightarrow e^+e^-$ events produced in association with a high p_T jet to examine the effects of strong radiative corrections. We have compared the primary jet pseudorapidity distribution, as a function of reconstructed W or Z boson rapidity to leading order (LO) and Next-to-Leading order (NLO) QCD Monte Carlo generators, as well as a model based on extended color dipoles. We find that the primary jet is more central than either LO or NLO expectations. None of the Monte Carlo programs does a good job of predicting the shape of the jet distributions as a function of intermediate vector bosons rapidity.

S. Abachi,¹² B. Abbott,³⁴ M. Abolins,²³ B.S. Acharya,⁴¹ I. Adam,¹⁰ D.L. Adams,³⁵ M. Adams,¹⁵
S. Ahn,¹² H. Aihara,²⁰ J. Alitti,³⁷ G. Álvarez,¹⁶ G.A. Alves,⁸ E. Amidi,²⁷ N. Amos,²²
E.W. Anderson,¹⁷ S.H. Aronson,³ R. Astur,³⁹ R.E. Avery,²⁹ A. Baden,²¹ V. Balamurali,³⁰
J. Balderston,¹⁴ B. Baldin,¹² J. Bantly,⁴ J.F. Bartlett,¹² K. Bazizi,⁷ J. Bendich,²⁰ S.B. Beri,³²
I. Bertram,³⁵ V.A. Bezzubov,³³ P.C. Bhat,¹² V. Bhatnagar,³² M. Bhattacharjee,¹¹ A. Bischoff,⁷
N. Biswas,³⁰ G. Blazey,¹² S. Blessing,¹³ P. Bloom,⁵ A. Boehnlein,¹² N.I. Bojko,³³
F. Borchering,¹² J. Borders,³⁶ C. Boswell,⁷ A. Brandt,¹² R. Brock,²³ A. Bross,¹² D. Buchholz,²⁹
V.S. Burtovoi,³³ J.M. Butler,¹² D. Casey,³⁶ H. Castilla-Valdez,⁹ D. Chakraborty,³⁹
S.-M. Chang,²⁷ S.V. Chekulaev,³³ L.-P. Chen,²⁰ W. Chen,³⁹ L. Chevalier,³⁷ S. Chopra,³²
B.C. Choudhary,⁷ J.H. Christenson,¹² M. Chung,¹⁵ D. Claes,³⁹ A.R. Clark,²⁰ W.G. Cobau,²¹
J. Cochran,⁷ W.E. Cooper,¹² C. Cretsinger,³⁶ D. Cullen-Vidal,⁴ M.A.C. Cummings,¹⁴ D. Cutts,⁴
O.I. Dahl,²⁰ K. De,⁴² M. Demarteau,¹² R. Demina,²⁷ K. Denisenko,¹² N. Denisenko,¹²
D. Denisov,¹² S.P. Denisov,³³ W. Dharmaratna,¹³ H.T. Diehl,¹² M. Diesburg,¹² G. Di Loreto,²³
R. Dixon,¹² P. Draper,⁴² J. Drinkard,⁶ Y. Ducros,³⁷ S.R. Dugad,⁴¹ S. Durston-Johnson,³⁶
D. Edmunds,²³ J. Ellison,⁷ V.D. Elvira,^{12,†} R. Engelmann,³⁹ S. Eno,²¹ G. Eppley,³⁵
P. Ermolov,²⁴ O.V. Eroshin,³³ V.N. Evdokimov,³³ S. Fahey,²³ T. Fahland,⁴ M. Fatyga,³
M.K. Fatyga,³⁶ J. Featherly,³ S. Feher,³⁹ D. Fein,² T. Ferbel,³⁶ G. Finocchiaro,³⁹ H.E. Fisk,¹²
Yu. Fisyak,²⁴ E. Flattum,²³ G.E. Forden,² M. Fortner,²⁸ K.C. Frame,²³ P. Franzini,¹⁰ S. Fuess,¹²
A.N. Galjaev,³³ E. Gallas,⁴² C.S. Gao,^{12,*} S. Gao,^{12,*} T.L. Geld,²³ R.J. Genik II,²³ K. Genser,¹²
C.E. Gerber,^{12,§} B. Gibbard,³ V. Glebov,³⁶ S. Glenn,⁵ B. Gobbi,²⁹ M. Goforth,¹³
A. Goldschmidt,²⁰ B. Gómez,¹ P.I. Goncharov,³³ H. Gordon,³ L.T. Goss,⁴³ N. Graf,³
P.D. Grannis,³⁹ D.R. Green,¹² J. Green,²⁸ H. Greenlee,¹² G. Griffin,⁶ N. Grossman,¹²
P. Grudberg,²⁰ S. Grünendahl,³⁶ W. Gu,^{12,*} G. Guglielmo,³¹ J.A. Guida,³⁹ J.M. Guida,³
W. Guryan,³ S.N. Gurzhiev,³³ P. Gutierrez,³¹ Y.E. Gutnikov,³³ N.J. Hadley,²¹ H. Haggerty,¹²
S. Hagopian,¹³ V. Hagopian,¹³ K.S. Hahn,³⁶ R.E. Hall,⁶ S. Hansen,¹² R. Hatcher,²³
J.M. Hauptman,¹⁷ D. Hedin,²⁸ A.P. Heinson,⁷ U. Heintz,¹² R. Hernández-Montoya,⁹
T. Heuring,¹³ R. Hirosky,¹³ J.D. Hobbs,¹² B. Hoeneisen,^{1,¶} J.S. Hoftun,⁴ F. Hsieh,²² Ting Hu,³⁹

¹Submitted XVII International Symposium on Lepton-Photon Interactions (LP95), Beijing, China, August 10-15, 1995.

Tong Hu,¹⁶ T. Huehn,⁷ S. Igarashi,¹² A.S. Ito,¹² E. James,² J. Jaques,³⁰ S.A. Jerger,²³
 J.Z.-Y. Jiang,³⁹ T. Joffe-Minor,²⁹ H. Johari,²⁷ K. Johns,² M. Johnson,¹² H. Johnstad,⁴⁰
 A. Jonckheere,¹² M. Jones,¹⁴ H. Jöstlein,¹² S.Y. Jun,²⁹ C.K. Jung,³⁹ S. Kahn,³ G. Kalbfleisch,³¹
 J.S. Kang,¹⁸ R. Kehoe,³⁰ M.L. Kelly,³⁰ A. Kernan,⁷ L. Kerth,²⁰ C.L. Kim,¹⁸ S.K. Kim,³⁸
 A. Klatchko,¹³ B. Klima,¹² B.I. Klochkov,³³ C. Klopfenstein,³⁹ V.I. Klyukhin,³³
 V.I. Kochetkov,³³ J.M. Kohli,³² D. Koltick,³⁴ A.V. Kostritskiy,³³ J. Kotcher,³ J. Kourlas,²⁶
 A.V. Kozelov,³³ E.A. Kozlovski,³³ M.R. Krishnaswamy,⁴¹ S. Krzywdzinski,¹² S. Kunori,²¹
 S. Lami,³⁹ G. Landsberg,¹² R.E. Lanou,⁴ J-F. Lebrat,³⁷ A. Leflat,²⁴ H. Li,³⁹ J. Li,⁴² Y.K. Li,²⁹
 Q.Z. Li-Demarteau,¹² J.G.R. Lima,⁸ D. Lincoln,²² S.L. Linn,¹³ J. Linnemann,²³ R. Lipton,¹²
 Y.C. Liu,²⁹ F. Lobkowicz,³⁶ S.C. Loken,²⁰ S. Lökös,³⁹ L. Lueking,¹² A.L. Lyon,²¹
 A.K.A. Maciel,⁸ R.J. Madaras,²⁰ R. Madden,¹³ I.V. Mandrichenko,³³ Ph. Mangeot,³⁷ S. Mani,⁵
 B. Mansoulié,³⁷ H.S. Mao,^{12,*} S. Margulies,¹⁵ R. Markeloff,²⁸ L. Markosky,² T. Marshall,¹⁶
 M.I. Martin,¹² M. Marx,³⁹ B. May,²⁹ A.A. Mayorov,³³ R. McCarthy,³⁹ T. McKibben,¹⁵
 J. McKinley,²³ T. McMahon,³¹ H.L. Melanson,¹² J.R.T. de Mello Neto,⁸ K.W. Merritt,¹²
 H. Miettinen,³⁵ A. Milder,² A. Mincer,²⁶ J.M. de Miranda,⁸ C.S. Mishra,¹²
 M. Mohammadi-Baarmand,³⁹ N. Mokhov,¹² N.K. Mondal,⁴¹ H.E. Montgomery,¹² P. Mooney,¹
 M. Mudan,²⁶ C. Murphy,¹⁶ C.T. Murphy,¹² F. Nang,⁴ M. Narain,¹² V.S. Narasimham,⁴¹
 A. Narayanan,² H.A. Neal,²² J.P. Negret,¹ E. Neis,²² P. Nemethy,²⁶ D. Nešić,⁴ D. Norman,⁴³
 L. Oesch,²² V. Oguri,⁸ E. Oltman,²⁰ N. Oshima,¹² D. Owen,²³ P. Padley,³⁵ M. Pang,¹⁷ A. Para,¹²
 C.H. Park,¹² Y.M. Park,¹⁹ R. Partridge,⁴ N. Parua,⁴¹ M. Paterno,³⁶ J. Perkins,⁴² A. Peryshkin,¹²
 M. Peters,¹⁴ H. Piekarz,¹³ Y. Pischalnikov,³⁴ A. Pluquet,³⁷ V.M. Podstavkov,³³ B.G. Pope,²³
 H.B. Prosper,¹³ S. Protopopescu,³ D. Pušeljčić,²⁰ J. Qian,²² P.Z. Quintas,¹² R. Raja,¹²
 S. Rajagopalan,³⁹ O. Ramirez,¹⁵ M.V.S. Rao,⁴¹ P.A. Rapidis,¹² L. Rasmussen,³⁹ A.L. Read,¹²
 S. Reucroft,²⁷ M. Rijssenbeek,³⁹ T. Rockwell,²³ N.A. Roe,²⁰ P. Rubinov,³⁹ R. Ruchti,³⁰
 S. Rusin,²⁴ J. Rutherford,² A. Santoro,⁸ L. Sawyer,⁴² R.D. Schamberger,³⁹ H. Schellman,²⁹
 J. Sculli,²⁶ E. Shabalina,²⁴ C. Shaffer,¹³ H.C. Shankar,⁴¹ R.K. Shivpuri,¹¹ M. Shupe,²
 J.B. Singh,³² V. Sirotenko,²⁸ W. Smart,¹² A. Smith,² R.P. Smith,¹² R. Snihur,²⁹ G.R. Snow,²⁵
 S. Snyder,³⁹ J. Solomon,¹⁵ P.M. Sood,³² M. Sosebee,⁴² M. Souza,⁸ A.L. Spadafora,²⁰
 R.W. Stephens,⁴² M.L. Stevenson,²⁰ D. Stewart,²² D.A. Stoianova,³³ D. Stoker,⁵ K. Streets,²⁶
 M. Strovink,²⁰ A. Taketani,¹² P. Tamburello,²¹ J. Tarazi,⁶ M. Tartaglia,¹² T.L. Taylor,²⁹
 J. Teiger,³⁷ J. Thompson,²¹ T.G. Trippe,²⁰ P.M. Tuts,¹⁰ N. Varelas,²³ E.W. Varnes,²⁰
 P.R.G. Virador,²⁰ D. Vititoe,² A.A. Volkov,³³ A.P. Vorobiev,³³ H.D. Wahl,¹³ G. Wang,¹³
 J. Wang,^{12,*} L.Z. Wang,^{12,*} J. Warchol,³⁰ M. Wayne,³⁰ H. Weerts,²³ F. Wen,¹³ W.A. Wenzel,²⁰
 A. White,⁴² J.T. White,⁴³ J.A. Wightman,¹⁷ J. Wilcox,²⁷ S. Willis,²⁸ S.J. Wimpenny,⁷
 J.V.D. Wirjawan,⁴³ J. Womersley,¹² E. Won,³⁶ D.R. Wood,¹² H. Xu,⁴ R. Yamada,¹² P. Yamin,³
 C. Yanagisawa,³⁹ J. Yang,²⁶ T. Yasuda,²⁷ C. Yoshikawa,¹⁴ S. Youssef,¹³ J. Yu,³⁶ Y. Yu,³⁸
 Y. Zhang,^{12,*} Y.H. Zhou,^{12,*} Q. Zhu,²⁶ Y.S. Zhu,^{12,*} Z.H. Zhu,³⁶ D. Zieminska,¹⁶ A. Zieminski,¹⁶
 and A. Zylberstejn³⁷

¹ Universidad de los Andes, Bogotá, Colombia

² University of Arizona, Tucson, Arizona 85721

³ Brookhaven National Laboratory, Upton, New York 11973

⁴ Brown University, Providence, Rhode Island 02912

⁵ University of California, Davis, California 95616

⁶ University of California, Irvine, California 92717

⁷ University of California, Riverside, California 92521

⁸ LAFEX, Centro Brasileiro de Pesquisas Físicas, Rio de Janeiro, Brazil

⁹ CINVESTAV, Mexico City, Mexico

¹⁰ Columbia University, New York, New York 10027

¹¹ Delhi University, Delhi, India 110007

¹² Fermi National Accelerator Laboratory, Batavia, Illinois 60510

- ¹³Florida State University, Tallahassee, Florida 32306
¹⁴University of Hawaii, Honolulu, Hawaii 96822
¹⁵University of Illinois at Chicago, Chicago, Illinois 60607
¹⁶Indiana University, Bloomington, Indiana 47405
¹⁷Iowa State University, Ames, Iowa 50011
¹⁸Korea University, Seoul, Korea
¹⁹Kyungsung University, Pusan, Korea
²⁰Lawrence Berkeley Laboratory and University of California, Berkeley, California 94720
²¹University of Maryland, College Park, Maryland 20742
²²University of Michigan, Ann Arbor, Michigan 48109
²³Michigan State University, East Lansing, Michigan 48824
²⁴Moscow State University, Moscow, Russia
²⁵University of Nebraska, Lincoln, Nebraska 68588
²⁶New York University, New York, New York 10003
²⁷Northeastern University, Boston, Massachusetts 02115
²⁸Northern Illinois University, DeKalb, Illinois 60115
²⁹Northwestern University, Evanston, Illinois 60208
³⁰University of Notre Dame, Notre Dame, Indiana 46556
³¹University of Oklahoma, Norman, Oklahoma 73019
³²University of Panjab, Chandigarh 16-00-14, India
³³Institute for High Energy Physics, 142-284 Protvino, Russia
³⁴Purdue University, West Lafayette, Indiana 47907
³⁵Rice University, Houston, Texas 77251
³⁶University of Rochester, Rochester, New York 14627
³⁷CEA, DAPNIA/Service de Physique des Particules, CE-SACLAY, France
³⁸Seoul National University, Seoul, Korea
³⁹State University of New York, Stony Brook, New York 11794
⁴⁰SSC Laboratory, Dallas, Texas 75237
⁴¹Tata Institute of Fundamental Research, Colaba, Bombay 400005, India
⁴²University of Texas, Arlington, Texas 76019
⁴³Texas A&M University, College Station, Texas 77843

The transverse momentum of a massive electroweak vector boson, either a W or Z boson, produced in $\bar{p}p$ collisions arises from multiple gluon emission. For sufficiently large transverse momentum it has been expected that the lowest order processes indicated in Fig. 1 play a predominant role. In both processes a single jet originating from one of the two incident parton lines is mainly responsible for compensating the massive boson's transverse momentum. These cross sections are maximized when the jet has the same rapidity as the intermediate vector boson. This relationship will be altered by the proton's structure functions which determine the probability of finding suitable initial partons to produce a given event topology.

This correlation between the jet's pseudorapidity, η , and the intermediate vector boson's rapidity could also be affected by several additional physical processes. For instance, gluons are expected to be radiated preferentially between the primary jet and the nearest beam. The recoil from these jets could systematically shift the original jet to more central rapidities. An alternative process, based on the extended color dipole model (1), would preferentially produce central gluon jets (2) independent of the intermediate vector boson's rapidity. The extended color dipole model assumes that all the color charges inside the incident proton can contribute to determining the radiation pattern for the primary jet. It then assumes that the coherent interference effects associated with the proton's finite transverse size limit

the available phase space and excludes gluon radiation at large rapidities.

We present a study of the rapidity correlation of a high p_T intermediate vector boson and the event's primary jet as a function of intermediate vector boson rapidity. We used W boson events identified in the $e\nu$ channel and Z boson events in the e^+e^- channel observed by the DØ detector. We do not distinguish between the different electron candidate charges. The resulting correlations were compared to the predictions from lowest order (3) (LO) and Next-to-Leading order (3) (NLO) QCD Monte Carlo generators, and ARIADNE (4), a model based on the extended color dipole. The NLO Monte Carlo program, DYRAD, is an order α_s^2 simulation.

This study is based on approximately 32 pb^{-1} for both the 1992-93 collider run and the 1994-95 collider run before January 1995. The DØ detector is described in detail elsewhere (5). We review here the features of the detector relevant for this analysis. Both the W and Z boson events were selected at the hardware trigger level by requiring a minimum of one electromagnetic (EM) trigger tower ($\Delta\eta \times \Delta\phi = 0.2 \times 0.2$) in the pseudorapidity range of $|\eta| \leq 3.2$ to have at least 10 GeV transverse energy or two such towers each with transverse energy above 7 GeV. The subsequent higher trigger levels required a cluster of EM cells with a transverse energy of 20 GeV as well as some rudimentary shape and isolation cuts. Additionally, the software trigger required that the $W \rightarrow e\nu$ events have a missing transverse energy, \cancel{E}_T , for the event in excess of 20 GeV. This missing transverse energy cut is increased to 25 GeV offline. The missing transverse energy vector, $\vec{\cancel{E}}_T$, is calculated using the hit information from the entire calorimeter, EM as well as hadronic, which covers pseudorapidity between ± 4 units.

The offline electron identification requires that the candidate shower have 90% or greater EM energy fraction and that an "H-matrix" analysis (6) of the shower shape be consistent with an electron. Furthermore, the candidate cluster must be isolated with $(E_{0.4} - EM_{0.2})/EM_{0.2} \leq 0.15$. The first term in the numerator, $E_{0.4}$, is the total energy (hadronic plus electromagnetic) in a cone of $\Delta R = \sqrt{\Delta\eta^2 + \Delta\phi^2} = 0.4$ centered on the electron candidate. The denominator, $EM_{0.2}$, is the electromagnetic energy inside the $\Delta R = 0.2$ cone. Finally, the electron candidate is required to have a charged track pointing toward the shower centroid. Only electron candidates with absolute pseudorapidity less than 1.1 or between 1.5 and 3.2 are used since this insures that they are well contained in the electromagnetic calorimeter. We also require that the electron candidates have transverse energy greater than 25 GeV when forming W or Z boson candidates. The magnitude of $\vec{\cancel{E}}_T$ is also required to be greater than 25 GeV for the $W \rightarrow e\nu$ reconstruction. The W boson candidates are then selected by requiring the transverse mass, M_T , formed by the electron candidate and the event's $\vec{\cancel{E}}_T$ to be greater than 45 GeV and less than 82 GeV. The final Z boson sample required that the invariant mass of the e^+e^- system be between 86 and 96 GeV/ c^2 .

This analysis also requires at least one jet with $p_T \geq 20 \text{ GeV}/c$ and with pseudorapidity between -3 and 3 units. The jets are found using a cone algorithm with $\Delta R = 0.7$. The jets must also pass cuts designed to remove calorimeter clusters resulting from spurious calorimeter hits. These jet quality cuts are 95% effective at removing spurious jets and remove only 4% of real jets. The electron isolation cut is further strengthened by requiring that the ΔR separation between any reconstructed jet and the electron candidates be greater than 1.1. Finally, we reduce the QCD background for both W and Z boson samples, which is dominated by back to back dijet events, by requiring that the difference in azimuthal angle between the leading jet and the electron candidates, $\Delta\phi_{ej}$, be less than 2.5 radians.

The rapidity of the $Z \rightarrow e^+e^-$ is unambiguously reconstructed since we use the

e^+e^- system's momenta to determine all the components of the Z boson's 4-vector. The $W \rightarrow e\nu$ system is, however, less well defined. In reconstructing the W boson's rapidity we constrain the decay's kinematics to the world average mass, $80.22 \text{ GeV}/c^2$ (7). For this procedure the transverse momentum of the W boson, $\vec{p}_T(W)$, is determined by the event's missing transverse energy, $\vec{\cancel{E}}_T$, plus the transverse momentum of the electron. The W boson's momentum component along the beam direction, $p_Z(W)$, is not directly measurable since a considerable fraction of the collision's energy escapes detection down the beam pipe. Instead, $p_Z(W)$ is estimated for each event during the mass constraint. We are left with, in general, two solutions for $p_Z(W)$. *A priori*, there are a number of ways of choosing the "correct" solution. Monte Carlo studies indicate that choosing the minimum $|p_Z(W)|$ produces a good estimate. This is the algorithm that we use for this analysis. Given both the $p_Z(W)$ and $\vec{p}_T(W)$ we may calculate the W boson rapidity by $y_W = \ln\sqrt{(E_w + P_z(W))/(E_w - P_z(W))}$. Figure 2 shows the distributions of reconstructed W boson rapidities from the final data sample as well as the electron pseudorapidity. The background contributions (see below) have been subtracted from both distributions. The ARIADNE and NLO predictions for the reconstructed W boson rapidity distribution are also shown. Both the NLO and ARIADNE do an acceptable job of predicting this distribution with the NLO doing a better job of predicting the fraction of central W bosons. We always use the same algorithms in reconstructing the Monte Carlo generated intermediate vector boson's rapidity as was used for the data. We have determined the y_W reconstruction resolution of our detector to be 0.097 ± 0.009 units of rapidity by considering the $Z \rightarrow e^+e^-$ sample and artificially removing one of the electrons from the event. The new $\vec{\cancel{E}}_T$ is then calculated and the event is subjected to the same procedure used in the W boson rapidity reconstruction algorithm, only now constraining the system to M_Z . This width is considerably smaller than the $\Delta y_W = 0.5$ bins that we use in the correlation study. We are not able to verify the Monte Carlo predictions for the fractional contributions of the actual y_W to each reconstructed y_W bin since $Z \rightarrow e^+e^-$ decays have a very different asymmetry from $W \rightarrow e\nu$ decays.

The backgrounds to both the $W \rightarrow e\nu + jets$ and $Z \rightarrow e^+e^- + jets$ are dominated by purely QCD processes where one or more of the jets fakes an electron. Monte Carlo studies indicate that processes involving real intermediate vector bosons but with the decay channel misidentified, such as $W + jets \rightarrow \tau\nu, \tau \rightarrow e\nu$ being identified as $W + jets \rightarrow e\nu$ contribute less than 4% of the sample at any reconstructed y_W . We determined the background from a sample of events taken with the same triggers used to collect the W and Z boson samples. These events were required to have either one or two "bad" electrons in order to be used in the W or Z boson background samples respectively. A bad electron consisted of an electromagnetic cluster which failed at least two of the three electron quality cuts but still satisfied the electron kinematic cuts. All other appropriate selection cuts were then applied to these background samples. The \cancel{E}_T distribution of W boson background sample was normalized to the signal sample below \cancel{E}_T of 20 GeV. The Z boson background sample was determined by normalizing the e^+e^- invariant mass distributions in the side bands, M_{ee} between 70 and 86 GeV/c^2 and 96 and 110 GeV/c^2 . The same rapidity reconstruction algorithms applied to the signal samples were then applied to the background samples. These procedures yielded a total of 1341 W boson candidates and 164 Z boson candidates with background fractions of 19% and 14% respectively.

The W and Z boson samples were then separately divided into five equal intervals of the absolute values of the reconstructed rapidity, either $|y_W|$ or $|y_Z|$, between 0. and 2.5. The pseudorapidity of each event's highest E_T jet was then plotted for each intermediate vector boson rapidity interval reconstructed where the sign of the jet rapidity was defined on an event-by-event basis as $\eta_{jet} \times y_{ivb}/|y_{ivb}|$. Thus jets with positive pseudorapidity are on the same side of the event as the intermediate vector boson while jets with negative pseudorapidity are on the opposite side. The average jet pseudorapidities, as a function of the intermediate vector boson's rapidity are shown in Fig. 3. The contributions to these averages from the backgrounds have been subtracted. The errors associated with these averages have been determined by propagating the errors for the average of

all candidate events and the weighted error of the average for the estimated background.

These indicate that the primary jet in these high p_T intermediate vector boson events is more central than either the LO or NLO predictions. We used the distribution of jets in each individual W boson rapidity bin to determine the significance of the shift. These are shown in Fig. 4. The background has been subtracted bin-by-bin and all the Monte Carlo generated events have been normalized to the total number of observed W bosons integrated over y_W . None of the Monte Carlo generators do a good job of reproducing the jet distributions. The probabilities that the discrepancies seen in Fig. 4 are due to statistical fluctuations alone are less than 10% for both ARIADNE and the NLO Monte Carlo program and less than 1% for the leading order prediction.

We varied the structure functions for the LO and NLO estimates using various modern sets; Morfin-Tung LO (8) and CTEQ2L (9) for the LO and CTEQ2M, CTEQ2MF, CTEQ2MS (9), MRSH, (10) and KMRSB0 (11) for the NLO. We saw only insignificant differences. We have also varied the energy scale for the LO structure functions between M_T^2 and $M_T^2/4$ without detecting a noticeable effect on the rapidity correlations. This insensitivity to the proton structure is expected given the large $Q^2 \approx M_W^2$ for these events. We ruled out η symmetric jet reconstruction inefficiencies by considering the ratio of jets on the same side as the W boson versus jets on the opposite side. Asymmetric η inefficiencies were eliminated by considering the production of jets with positive lab frame η (here defined as the direction of the incident proton) relative to those with negative lab frame η . We have also tried changing our definition of “primary” jet to be the jet with $|p_T|$ closest to the p_T of the intermediate vector boson’s transverse momentum with no noticeable effect. It should be pointed out that the transverse momentum of the intermediate vector bosons are highly correlated with the primary jet when using either of these definitions. This implies that additional radiation is not playing a major role.

Finally, we have examined the dependence of our measurements on the algorithm for determining the rapidity of the W . We have tried both unfolding these mistakes on the data directly and using a weighting scheme without noticeable changes in our final distributions.

In conclusion, we have studied the rapidity correlation between the reconstructed intermediate vector boson and the event’s highest p_T jet. None of the models for high p_T intermediate vector boson production in $p\bar{p}$ collisions do a particularly good job of reproducing the observed behavior of the data in that the primary jet remains central, independent of the intermediate vector boson’s reconstructed rapidity. The model based on extended color dipoles does the best job of predicting the W boson-jet correlation.

ACKNOWLEDGMENTS

We thank the Fermilab Accelerator, Computing, and Research Divisions, and the support staffs at the collaborating institutions for their contributions to the success of this work. We also acknowledge the support of the U.S. Department of Energy, the U.S. National Science Foundation, the Commissariat à l’Energie Atomique in France, the Ministry for Atomic Energy and the Ministry of Science and Technology Policy in Russia, CNPq in Brazil, the Departments of Atomic Energy and Science and Education in India, Colciencias in Colombia, CONACyT in Mexico, the Ministry of Education, Research Foundation and KOSEF in Korea and the A.P. Sloan Foundation.

We would like to thank B. Andersson whose many interesting conversations stimulated this study. We are also grateful to L. Lönnblad for providing us the ARIADNE Monte Carlo program for simulating high p_T intermediate vector boson events using the extended color dipole model and to W. Geile for his help in running the NLO Monte Carlo program, DYRAD.

REFERENCES

* Visitor from IHEP, Beijing, China.

‡ Visitor from CONICET, Argentina.

§ Visitor from Universidad de Buenos Aires, Argentina.

¶ Visitor from Univ. San Francisco de Quito, Ecuador.

1. B.Andersson, G. Gustafson, L. Lönnblad, U. Petterson, *Z. Phys. C* **43**, 625-632 (1989)
2. B. Andersson, Private Communication
3. W.T. Giele, E.W.N. Glover, D. A. Kosower *Phys. Lett. B***309** 205 (1993)
4. L. Lönnblad, *Comp. Phys. Comm.* **71** 15 (1992). We have used ARIADNE version 4.05P02 in this analysis.
5. S. Abachi *et al.*, *Nucl. Instr. and Meth. in Phys.* **A338** 185 (1994)
6. R. Engelmann *Nucl. Instr. Meth.* **216** 45 (1983); M. Narain, 7th Meeting of the APS Divisions of Particles and Fields, C. H. Albright ed. World Scientific, Batavia Il. (1992)
7. K. Hikasa *et al.*, *Phys. Rev. D* **45** (1992)
8. J. Morfin and W.K. Tung, *Z. Phys.* **C52** 13 (1991)
9. J. Botts *et al.*, *Phys. Lett.* **304B** 159 (1993)
10. A.D. Martin, R.G. Roberts, and W.J. Stirling, *Proc. Workshop on Quantum Field Theoretical Aspects of High Energy Physics*, Kyffhäuser, Germany, eds. B. Geyer and E.-M. Ilgenfritz, Leipzig (1993) p. 11
11. J. Kwiecinski, A.D. Martin, R.G. Roberts and W.J. Stirling, *Phys. Rev. D***42** 3645 (1990)

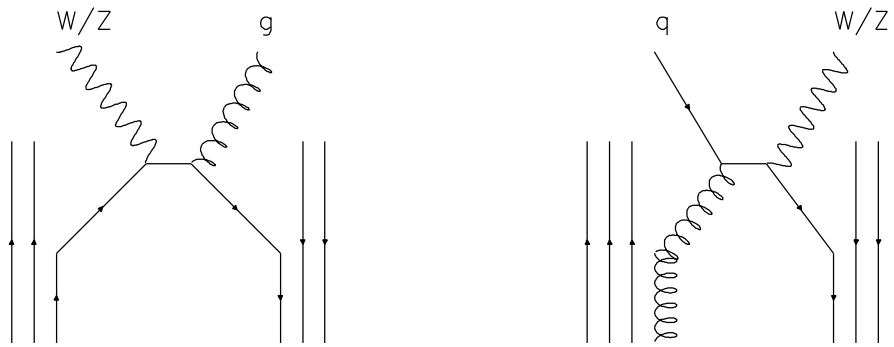


FIG. 1. The two dominant lowest order processes, the annihilation and Compton diagrams, yielding high p_T W bosons.

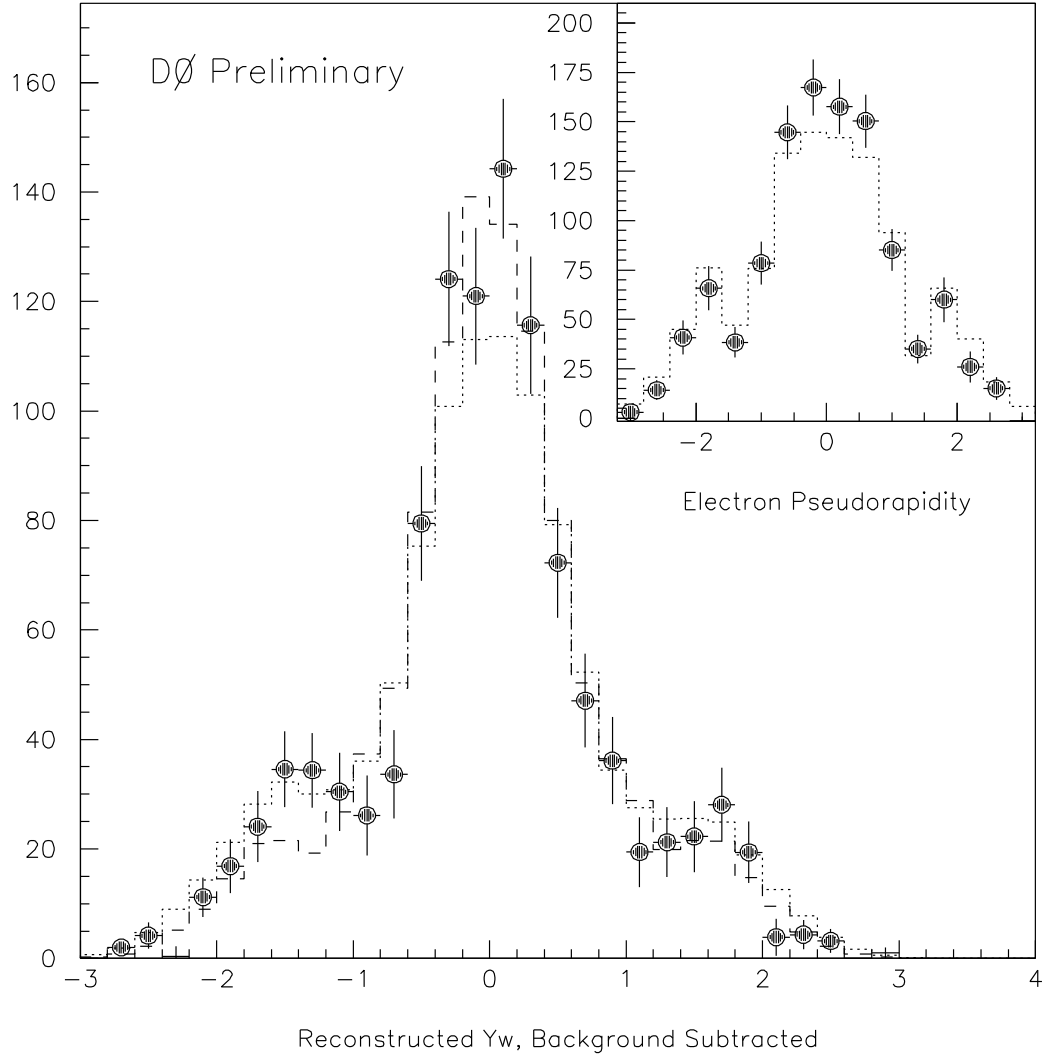


FIG. 2. The distribution of reconstructed W boson rapidities is shown together with the color dipole (dotted line) and the Next-to-Leading order (dashed line) expectations. The insert shows the electron pseudorapidity distribution and the color dipole (dotted line) prediction for this quantity. The background contributions have been subtracted from both distributions.

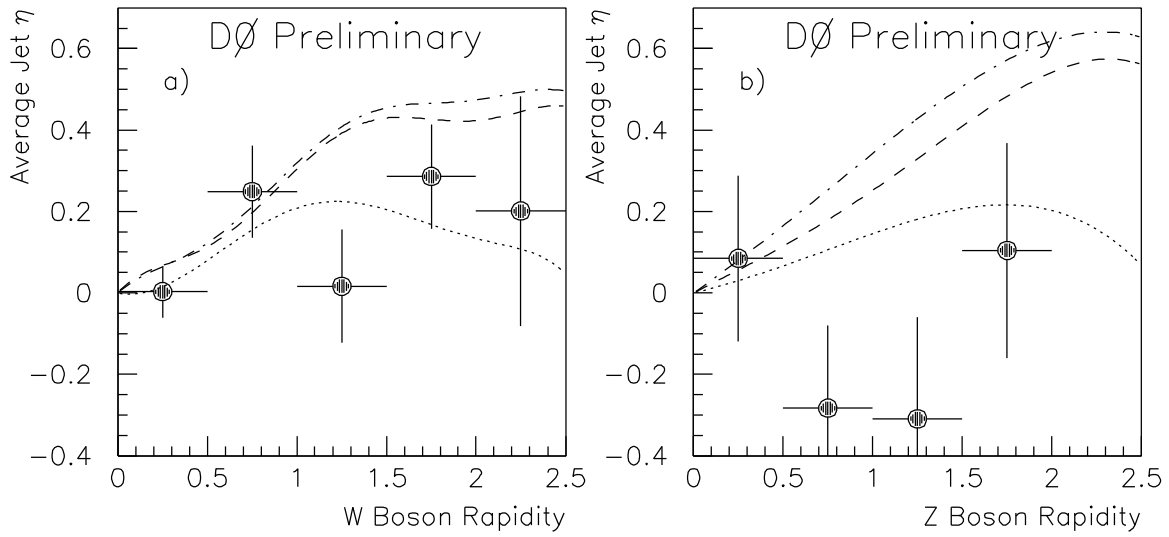


FIG. 3. The average jet pseudorapidity relative to the intermediate vector bosons (see text for explanation) is shown as a function of reconstructed W boson rapidity in figure 3a and Z boson rapidity in figure 3b. The Leading Order (dot-dashed lines), Next-to-Leading order (dashed lines), and Extended Color Dipole (dotted lines) expectations for these averages are also shown.

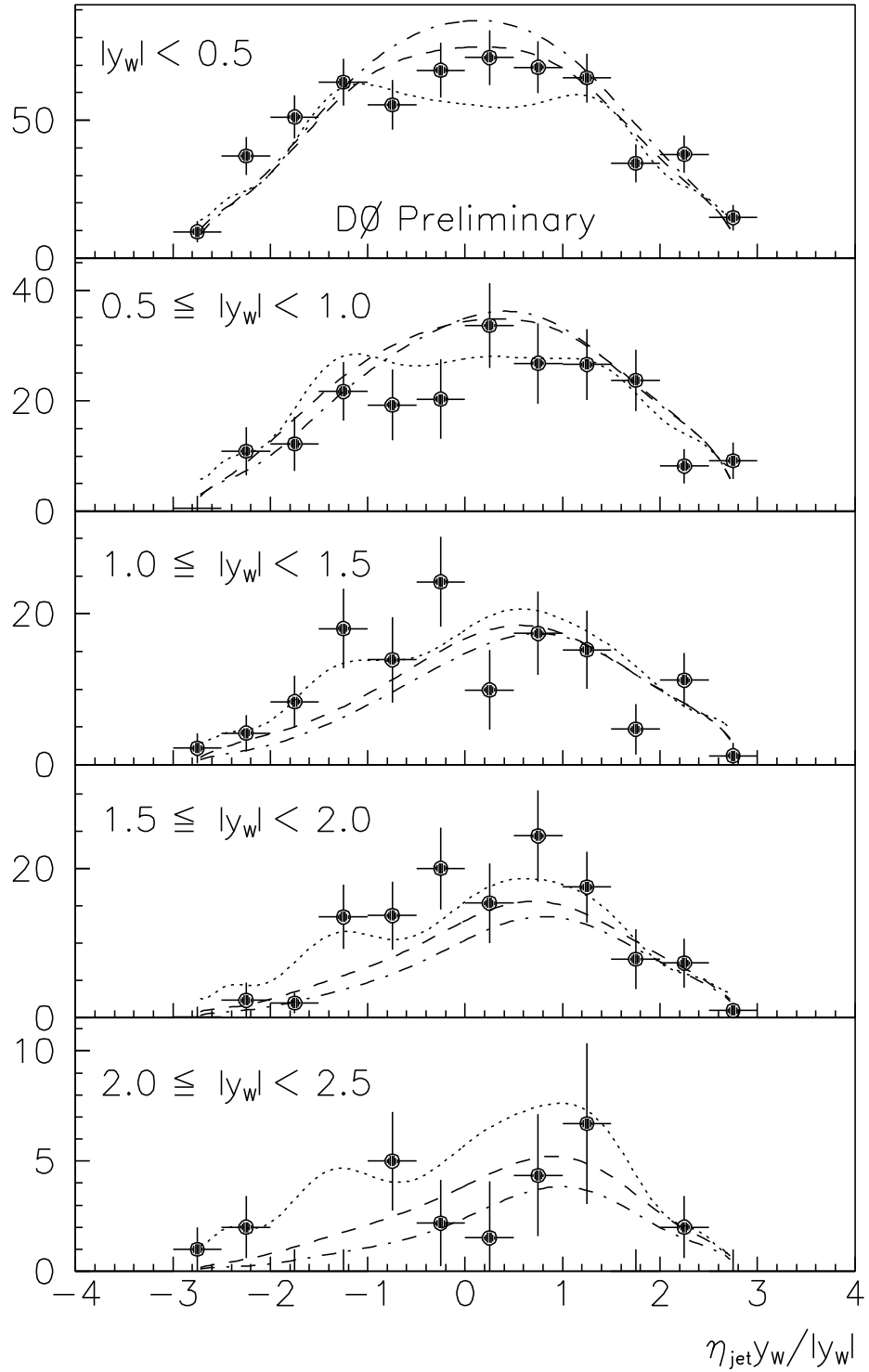


FIG. 4. The distributions of pseudorapidity of the leading E_T jets in W boson events are shown for the five intervals of y_W less than 2.5. The three different Monte Carlo expectations, ARIADNE — dotted lines, DYRAD NLO — dashed, and LO — dot-dashed lines are also shown.